Title
Genetic deletion of CD36 enhances injury after acute neonatal stroke

Journal
Annals of Neurology, 72(6)

ISSN
0364-5134

Authors
Woo, Moon-Sook
Wang, Xia
Faustino, Joel V
et al.

Publication Date
2012-12-01

DOI
10.1002/ana.23727

Peer reviewed

Published in final edited form as:
Ann Neurol. 2012 December ; 72(6): 961–970. doi:10.1002/ana.23727.

Genetic deletion of CD36 enhances injury after acute neonatal stroke

Moon-Sook Woo, PhD[1,*], **X. Wang, MD**[1,2,*], **Joel V. Faustino, BS**[1,*], **Nikita Derugin, MA**[1], **Michael F. Wendland, PhD**[3], **Ping Zhou, PhD**[4], **Costantino Iadecola, MD**[4], and **Zinaida S. Vexler, PhD**[1]

[1]Department of Neurology, University of California, San Francisco, San Francisco, CA

[2]Department of Pediatrics, Xiangya Hospital, Central South University, China

[3]Department of Radiology, University of California, San Francisco, San Francisco, CA

[4]Neurology and Neuroscience, Weill Cornell Medical College, New York, NY

Abstract

OBJECTIVES—The scavenger receptor CD36 is injurious in acute experimental focal stroke and neurodegenerative diseases in the adult. We investigated the effects of genetic deletion of CD36 (CD36ko) on acute injury, and oxidative and inflammatory signaling after neonatal stroke.

METHODS—P9 CD36ko and wild type (WT) mice were subjected to a transient middle cerebral artery occlusion (MCAO). Injury, phagocytosis of dying cells, and CD36 inflammatory signaling were determined.

RESULTS—While the volume of "tissue at risk" by diffusion-weighted MRI during MCAO was similar in neonatal CD36ko and WT mice, by 24 hrs after reperfusion, injury was more severe in CD36ko and was associated with increased caspase-3 cleavage and reduced engulfment of neurons expressing cleaved caspase-3 by activated microglia. No significant superoxide generation was observed in activated microglia in injured WT whereas increased superoxide production in vessels and NFκB activation induced by MCAO were unaffected by lack of CD36. While Lyn expression was higher in injured CD36ko, cell-type specific patterns of Lyn expression were altered; Lyn was expressed in endothelial cells and microglia in WT but predominantly in dying neurons in CD36ko.

Interpretation—Lack of CD36 results in poorer short-term outcome from neonatal focal stroke due to lack of attenuation of NFκB-mediated inflammation and diminished removal of apoptotic neuronal debris. While inhibition of CD36 does not seem to be a good therapeutic target for protection after acute neonatal stroke, like it is after adult stroke, seeking better understanding of CD36 signaling in particular cell populations may reveal important therapeutic targets for neonatal stroke.

Keywords

Neonatal stroke; microglia; caspase-3; superoxide; cytokine; NF-κB, Src kinase, Lyn

Corresponding Author: Zinaida S. Vexler, Ph.D. University California San Francisco Department of Neurology, box 0663 521 Parnassus Ave. San Francisco, CA 94143-0663 Tel (415) 502-2282 Fax (415) 502-5821 Zena.Vexler@ucsf.edu.
[*]these authors equally contributed to the study.

Disclosures
None

Introduction

The scavenger receptor CD36 is a transmembrane glycoprotein that participates in multiple biological functions, such as production of reactive oxygen species (ROS), uptake of oxLDL and long chain fatty acids, chemotaxis of immune cells [1], foam cell formation [2], and phagocytosis of apoptotic cells [3]. It also serves as an anti-angiogenic factor [4]. CD36 is expressed by several cell types, including monocytes, microglia and endothelial cells [5] and exerts its cell-type specific effects through multiple ligands or acts via cooperation with other receptors, thereby modulating intracellular signaling pathways through the clustered receptors [6, 7]. There is extensive evidence that CD36 mediates Aβ toxicity, oxLDL-atherosclerosis and injury after stroke [1, 2, 8]. In all of these cases, CD36 triggers production of superoxide, which then serves as an injury mediator [2, 8, 9]. CD36-mediated superoxide production in $CD11b^+$ microglia/macrophages leads to injury after adult stroke: infarcts are reduced in CD36ko mice [8] or following pharmacological inhibition by SS31 [10]. The effects of CD36, however, are context-dependent, and CD36 is beneficial after intracerebral hemorrhage by mediating hematoma resolution through phagocytosis of red blood cells by microglia/macrophages[1112].

Although neonatal and adult stroke have a similar incidence [13], the injury mechanisms of neonatal stroke are vastly different from those of adult stroke, including the impact and mechanisms of neuroinflammation [14]. Immaturity during the early postnatal period makes the brain susceptible to ischemic, excitotoxic and oxidative damage [15, 16]. Microglial cells/macrophages are thought to contribute to injury after stroke in adults in part by producing inflammatory cytokines [14], but in neonatal stroke pharmacologic depletion of microglia further enhances cytokine and chemokine production and enhances injury [17]. Oxidative stress and inflammation are tightly linked. Once activated, the inflammatory cells generate ROS, which, in turn, can further amplify an inflammatory response and negatively impact phagocytosis of apoptotic debris, a prominent and distinct feature of the pathophysiology of hypoxia-ischemia (H-I) and focal stroke in neonates [18, 19]. The abundance of apoptotic neurons in acutely injured neonatal brain can be related to neuroinflammation either directly or indirectly. Considering that CD36 can enhance brain injury by inducing oxidative stress but protect by phagocytosing apoptotic cells [20, 21], we investigated the effects of genetic deletion of CD36 (CD36ko) on acute injury after neonatal stroke. We report that genetic deletion of CD36 results in poorer short-term outcome from transient middle cerebral artery occlusion (MCAO) induced in postnatal day 9 (P9) mice due to lack of attenuation of NFκB-mediated inflammation, changed signaling of the Src kinase Lyn and diminished removal of apoptotic neuronal debris.

Materials and Methods

Animals

All animal experiments were approved by the Institutional Animal Care and Use Committee of the University of California, San Francisco.

Transient 3 hour MCAO was induced in unsexed P9 mice in a manner similar to previously detailed in P7 rat [22], with modifications [23], are described in the Supplementary Methods.

DWI was performed using a 2T magnet with a Bruker Omega system to identify injured animals and determine the volume of "tissue at risk" ~2.5 hours after MCAO, as described [23].

Genotyping was performed as previously described [6].

Histological methodology, immunofluorescence and 3D data analysis of fluorescence data are described in the Supplementary Methods.

Superoxide production was determined in perfusion-fixated brains following administration of a cell-permeable dye, dihydroethidium (DHE, 5 mg/kg, i.p., 3 hours before sacrifice), as described [17]. The total number of Ox-DHE$^+$ cells and the number of Iba1$^+$/Ox-DHE$^+$ and IB4$^+$/Ox-DHE$^+$ cells were determined in 3D-reconstructed images [17].

Western Blot analysis in whole cell lysates, and nuclear and cytoplasmic fractions are described in the Supplementary Methods.

Electrophoretic mobility shift assay (EMSA) was performed to determine nuclear factor (NF)-κB binding activity in nuclear extracts (5 μg/sample) using a commercially available kit (Signosis). The position of NF-κB subunits was confirmed in competition assay by pre-incubating nuclear extracts with non-labeled NF-κB probes (1x-10x dilution). Supershift assay was performed by pre-incubating nuclear extracts with antibodies against p65 and p50 (6 μg/sample; Santa Cruz).

Reverse Transcription-Polymerase Chain Reaction (RT-PCR) is described in the Supplementary Methods.

Chemokine concentrations were measured in injured and contralateral tissue using a LINCOplex™ mouse cytokine multiplex (LINCO Research) as described [24].

Statistical Analysis

Data are presented as mean ± SD or as medians. Comparisons between two groups were statistically evaluated by the Student's t test. Differences were considered significant at $p < 0.05$.

Results

Genetic deletion of CD36 exacerbates acute injury after MCAO in neonatal mice

Injured P9 CD36ko and WT mice were selected based on DWI during MCAO [19, 23]. During MCAO, volumes of injury on DWI ("tissue at risk") were similar in CD36ko and WT, 64±12% and 60±14% of ipsilateral hemisphere, respectively (Fig. 1A, D). At 24 hours after reperfusion, the average injury volume on Nissl-stained sections in the same mice was significantly larger in CD36ko (48.7±6.1%) than in WT (29±30%; Fig. 1D, p=0.003). Volumes of injury on DWI and histology were similar in 90% of CD36ko mice, but only in 50% of WT mice (Figure 1E). Injury was limited to the caudate in the remaining WT mice, demonstrating a poorer recovery in mice that lack CD36. Severity of histological injury depended on the duration of MCAO (Supplementary Results, Suppl Fig1A).

Considering the known role of CD36 in removal apoptotic cells [21, 25] and caspase-3 being a major chemoattractant signal for phagocytosing cells [26], next we investigated the effect of CD36 on caspase-3-mediated and calpain-mediated cleavage of the structural protein spectrin. The extent of calpain-mediated spectrin cleavage (145/150kDa band, Fig. 1F,G) and caspase-3 mediated cleavage (120kDa band, Fig. 1F,H) varied in individual animals, with no statistical difference between the groups. Protein expression level of cleaved caspase-3 was, however, significantly higher in injured tissue of CD36ko (Fig. 1I, p=0.014).

A more marked presence of cleaved caspase-3 in CD36ko pups is associated with diminished engulfment of apoptotic neurons

To determine if lack of CD36 adversely affects removal of apoptotic debris, we first quantified the number and morphological characteristics of caspase-3^+ cells (cl.casp-3^+ cells) in the cortical penumbra, the ischemic core, and the injured caudate nucleus (regions defined by the DAPI morphology) 24 hours after MCAO (Fig. 2A,E), a time of profoundly increased caspase-3 activation [19]. As expected, cl.casp-3^+ cells were rarely seen in uninjured tissue, but casp-3 cleavage was consistently observed in injured regions (Fig. 2A,C). Cells with cl.casp-3 were at more advanced degradation stages in WT than in CD36ko (SupplFig. 1B-C).

We then determined engulfment of cl.casp-3^+ cells by activated microglia. Lack of CD36 did not affect the morphological characteristics of activated microglia (SupplFig. 2A-C) or the vessel size distribution and volume (SupplFig. 2D). However, the number of cl.casp-3^+ cells that either touched or were engulfed by $IB4^+$ cells was significantly higher in the injured caudate of WT mice (Fig. 2D), the most consistently and severely injured region in our model. Additional analysis of cl.caspase-3^+ cells distant or within $IB4^+$ vessels (Supplementary Materials) showed only few cl.casp-3^+ cells within vessels but significantly higher number of cl.casp-3^+/$IB4^+$ cells apart from the vessels (i.e., activated microglia) in WT mice. Together, these results suggest that lack of CD36 diminishes removal of apoptotic neuronal debris, thereby contributing to secondary necrosis and injury.

Superoxide accumulation in activated microglia/macrophages is low and is unaffected by lack of CD36 in acutely injured neonatal mice

In adults, free radical production in microglia/macrophages within 24 hours after MCAO contributes to injury in a CD36-dependent manner; reduced accumulation of Ox-DHE^+ protects CD36ko mice [8]. Application of the same method showed essentially no Ox-DHE^+ cells in both hemispheres 30min, 1, 3 and 6 hours after MCAO as well as in contralateral and uninjured ipsilateral tissue 24 hours after MCAO. The number of Ox-DHE^+ cells was similarly increased in injured cortex and caudate of WT and CD36ko (Fig. 3A,D). The majority of Ox-DHE^+ cells were seen in the vessels (Fig. 3A,B), and the rarely observed Ox-DHE signal was seen in vesicles of $Iba1^+$ cells (Fig. 3C,E), consistent with our previous findings in rat pups subjected to MCAO [17]. The number of Ox-DHE^+ activated microglia was similar in WT and CD36ko pups (Fig. 3E). Thus, the cellular sources of superoxide production and the corresponding injury mechanisms are different in acutely injured neonates and adults.

Lack of CD36 does not suppress NFκB activation or chemokine accumulation 24 hours after injury

NFκB binding was significantly increased by 24 hours in nuclear extracts from injured regions (injury confirmed by spectrin cleavage) compared to contralateral regions in each group (Fig. 4A,B, bands *a* and *b*). However, NFκB activation was unaffected by lack of CD36 at this point. The specificity of NF-κB binding and band identify were confirmed in competition and suprshift assays (Fig. 4C). Purity of the nuclear and cytosolic fractions was confirmed by an anti-histone H1 antibody (Fig. 4D). NFκB activation was associated with markedly decreased p65 and modestly reduced p50 in the cytosol, but the effect was independent of CD36 (Fig. 4D). A variable extent of increased p50 was observed in the nucleus in injured regions (Fig. 4E) but no increase of p65 expression was seen in the nucleus in injured regions of WT and CD36ko (Fig. 4F), likely due to degradation of p65. At 24 hours, the levels of MIP-1α (45.2±41.7 vs 18.8±6.6 pg/mg protein), MCP-1 (222.3±120.5 vs 32.1±30.8 pg/mg protein) and KC (290.1±175.9 vs 17.8±23.6 pg/mg protein) were significantly increased in injured Vs. contralateral regions, but changes were

similar in CD36ko (n=5/group). Therefore, NFκB activation and the levels of microglial and leukocyte chemoattractants were increased in acutely injured brains regardless of lack of CD36.

The cell-type specific patterns of Lyn expression depend on CD36

Finally, we asked if Src kinase activation, which mediates CD36 injury in mouse and human macrophages [1], is affected by lack of CD36. Lyn expression was similar in naïve WT and CD36ko in WCL (not shown) and remained unchanged 1 hour after reperfusion (Fig. 5B). At 24 hours, Lyn expression measured in WCL was significantly decreased in injured WT, but was better preserved in injured CD36ko (Fig. 5A,B). Consistently, Lyn-dependent signaling was significantly reduced in WT but not CD36ko (Supplementary Results, Suppl.Fig 3A). The reduced Lyn protein levels were not due to reduced transcriptional levels (Fig. 5C-D). CD36-dependent Lyn signaling may differ in cells of different origin [27, 28]. We found that in contralateral hemisphere of WT mice Lyn was ubiquitously expressed in the vessels (Fig. 5E-F) and in a subpopulation of microglial cells (Fig. 5E-F). The number of Lyn positive activated microglial cells was significantly increased in injured regions (Fig. 5E), consistent with its known role in cells of monocyte lineage. However, in contralateral hemisphere of CD36ko detectible levels of Lyn were evident only in a subpopulation of endothelial cells and an altered pattern of intracellular expression was seen in some $Iba1^+$ cells, in the nucleus and in the cytosol (Fig. 5E). Strikingly, in injured regions of CD36ko mice Lyn was localized predominantly in the nuclei of dying cells (Fig, 5E,G). Therefore, genetic deletion of CD36 modifies the cell-type specific Lyn expression and injury in neonatal brain.

Discussion

We report that genetic deletion of the scavenger receptor CD36 exacerbates injury after acute focal stroke in neonatal mice, an effect opposite to the reduced injury reported in adult mice after acute focal stroke [8]. We further show that, consistent with the differing effect of CD36 deletion on injury between neonates and adults, two key contributing mechanisms of CD36-mediated toxicity in adult post-ischemic brains—superoxide production in activated microglia/macrophages and NFκB activation—are unaffected by lack of CD36 in acutely injured neonatal brains. Lack of CD36 causes cell-type specific changes in Lyn expression; reduced expression in endothelial cells and macrophages but markedly increased accumulation in the nuclei of dying cells. Finally, we demonstrate that lack of CD36 adversely affects removal of apoptotic cells, enhancing injury.

Although volumes of “tissue at risk”, delineated by DWI during MCAO, are similar in neonatal CD36ko and WT mice, volume of histological injury is significantly larger in CD36ko pups and a more severe injury is associated with the altered balance between the apoptotic and excitotoxic injury components at 24 hours. While factors other than CD36 mediate phagocytosis [29], uniquely, CD36 contributes to several phagocytotic steps, including the recognition, engulfment and digestion of apoptotic cells [8, 20, 21]. CD36 plays a key role in phagocytosis of apoptotic neurons [20]. Overexpression of CD36 in cells with limited capacity to phagocytose apoptotic bodies markedly increases the uptake of various types of apoptotic cells [3]. Blockade of this receptor is substantially more effective in disrupting the uptake of apoptotic PC12 cells than blockade of lectin- or PS-mediated uptake [20]. In neonatal post-ischemic brain, the magnitude of caspase-3 mediated neuronal death is considerably higher than in adult post-ischemic brain [30], and the rate of apoptotic debris removal by phagocytosis is relatively low [17], which contributes to injury [19] and predisposes to neuroinflammation [24]. Insufficient clearance of apoptotic cells is injurious [31]. Thus, further diminished removal of dying cells in injured CD36ko and the associated

accumulation of cl.caspase-3 and enhanced caspase-3 dependent spectrin cleavage may account for injury exacerbation in immature CD36ko brain.

CD36 is central to several aspects of microglia/macrophage function, including migratory activity of these cells and production of inflammatory mediators [32, 33]. We therefore anticipated that the number of $Iba1^+$ cells would be unchanged and the cells would be smaller in CD36ko. Opposite to our expectations, the surface of $Iba1^+$ cells was larger and the number of $Iba1^+$ cells was higher in injured CD36ko. While there is no immediate explanation for these results, the phenotypes of $Iba1^+$ cells are likely to be different in injured neonates than in adults. Peripheral monocytes contribute significantly to CD36-induced brain injury in response to $A\beta_{1\text{-}40}$ [9] and hyperlipidemia [34] in the adult, whereas monocyte infiltration is low in acutely injured neonatal brain and macrophages mostly consist of activated microglia, as we showed by $CD45^{low/medium}/CD45^{high}$ expression in our model [24]. CD36 is also known to mediate macrophage fusion, leading to foam macrophage formation under hyperlipidemic conditions [32], but this mechanism is not applicable to neonatal brains. Proliferation of microglia and CD36-independent migratory activity of these cells, along with different oxidative metabolism in these cells, may account for the observed effects.

In fact, we show that the patterns of CD36-mediated superoxide accumulation after neonatal stroke are fundamentally different from those observed in several types of injury in the adult. Superoxide production in microglia, monocytes, neutrophils, and endothelial cells plays a key role in CD36 toxicity, both in vivo and in vitro [8, 35, 369]. Decreased CD36-dependent superoxide production in $CD11b^+$ microglia/macrophages is protective [8, 10, 36]. Our data in both neonatal rats [17] and mice consistently show that superoxide accumulation, which is increased in the vasculature within injured regions, but is modest and discrete in activated microglia, is independent of CD36. While the exact mechanisms of such striking age-dependant differences are largely unknown, the pattern of changes for CD36 and its downstream effectors after injury provides some clues. In the adult, CD36 toxicity depends on superoxide produced through NADPH oxidase (Nox) activation [9, 37], but the relative contribution of individual Nox isoforms [38] and superoxide utilization [39] after H-I in neonates differs from that after focal stroke in adults. The magnitude of CD36 upregulation may be critical as the injury modifier. Although both lack of CD36 or its marked upregulation exacerbate injury after neonatal stroke, a 2-fold increase in CD36 expression is not associated with increased superoxide production in microglia, whereas a 7-fold CD36 up-regulation (induced by altered redox metabolism in activated microglia before neonatal stroke) is associated with initiated superoxide production, leading to injury exacerbation, rearranged lipid rafts and enhanced cytokine production [17], a pattern that somewhat mirrors CD36-mediated superoxide-dependent injurious phenotype seen in injured adult brain.

We provide the first evidence that lack of CD36 reshapes the pattern of Lyn expression in multiple cells types after neonatal stroke. CD36 may signal through several Src kinases and downstream MAP kinases [2440], depending on cell types. Lyn, which is expressed in most hematopoietic cells and in several cell types in the brain [5], signals distinctly, depending on its intracellular localization. Our data shows that in injured regions of WT mice Lyn expression and signaling are significantly reduced while Lyn transcript levels are unchanged, suggesting its post-transcriptional down-regulation/proteosomal degradation. Intracellular redistribution of Lyn in CD36ko also suggests that CD36 controls the pattern of Lyn expression. At least two independent mechanisms can account for Lyn translocation into the nucleus. Lyn anchoring to the lipid fraction of the plasma membrane occurs through its structural N-terminal domain, a domain that contains myristylated (Gly2) and palmitoylated (Cys3) sites [41]. Mutations in these sequences, or lack or cleavage of N-terminal by activated caspases dissociate Lyn, cause its translocation into the cytosol and the

nucleus [42], alter intracellulal trafficking and activity in multiple cell types [4, 43] and contribute to apoptosis [4, 43]. Thus, enhanced caspase-3 may cleave Lyn and contribute to its translocation, but we rarely observed cleaved Lyn (double bands on Western). Lost Lyn interaction with CD36 in lipids is an alternative way for its translocation from the plasma membrane. While data are conflicting on whether CD36 physically interacts with Lyn [2, 7], or associates with Lyn through a hydrophobic interaction within lipid rafts [44], lack of CD36-Src interaction within lipids may disrupt multiple downstream signaling pathways, such as integrin or TLR signaling, as was shown for Aβ or oxLDL [7, 36].

NFκB regulates expression of multiple genes involved in inflammation, cell survival or apoptotic death. In contrast to adult stroke, where CD36-dependent NFκB activation mediates injury [37], while MCAO induces NFκB activation in neonates, its activation and the production of NFκB-dependent leukocyte chemoattractants are not significantly affected in CD36ko, at least within 24 hours. The role of NFκB in neonatal brain following H-I is complex. Early and transient pharmacological disruption of the IKK-NFκB complex causes potent protection [45], attenuated microglial activation and cytokine production after H-I [46], whereas sustained inhibition of this pathway for 24 hours not only completely abolishes protection but aggravates injury [46]. Thus, the dynamic nature of injury modulation by the NFκB originates from relatively independent signaling in different cell types, a notion consistent with our data on altered cell-type specific patterns of Lyn expression in CD36ko. The tight link between NFκB and ROS production in injured adults [8] but not in neonates is another plausible explanation for age-dependent effects of CD36 on NFκB activation. Finally, NFκB activation is in part attributed to infiltrated neutrophils in the adult [8] but neutrophil infiltration is negligible in our model [47].

To summarize, in this first study addressing the role of the scavenger receptor CD36 in neonatal stroke, we demonstrate strikingly different effects of this receptor compared to those reported in adult stroke. Although CD36-mediated effects in injured neonatal brains are complex and are far from being understood, the differing responses of the immature brain to ischemic injury, including the mechanisms of cell death, oxidative stress and inflammation, may in part occur through CD36 signaling. While inhibition of CD36 does not seem to be a good therapeutic target for acute neuroprotection after neonatal stroke, like it is after stroke in the adult, the diverse pattern of CD36 expression conveys its multiple cellular functions. Seeking better understanding of its signaling in particular cell populations, alone or in cooperation with other receptors, may reveal important therapeutic targets for neonatal stroke.

Supplementary Material

Refer to Web version on PubMed Central for supplementary material.

Acknowledgments

The authors acknowledge Baomei Liu for technical help during earlier stages of the project and Dr. Xiangning Jiang for useful discussions. The work was supported by RO1 NS55915 (Z.S.V), RO1 NIH NS44025 (Z.S.V), AHA GIA 0855235F (Z.S.V), RO1 NS34179 (C.I.), R01 NS73666 (C.I.), R01 NS67078 (P.Z.).

REFERENCES

1. Park YM, Febbraio M, Silverstein RL. CD36 modulates migration of mouse and human macrophages in response to oxidized LDL and may contribute to macrophage trapping in the arterial intima. J Clin Invest. 2009; 119:136–145. [PubMed: 19065049]
2. Rahaman SO, Lennon DJ, Febbraio M, et al. A CD36-dependent signaling cascade is necessary for macrophage foam cell formation. Cell Metab. 2006; 4:211–221. [PubMed: 16950138]

3. Ren Y, Silverstein RL, Allen J, Savill J. CD36 gene transfer confers capacity for phagocytosis of cells undergoing apoptosis. J Exp Med. 1995; 181:1857–1862. [PubMed: 7536797]
4. Jimenez B, Volpert OV, Crawford SE, et al. Signals leading to apoptosis-dependent inhibition of neovascularization by thrombospondin-1. Nat Med. 2000; 6:41–48. [PubMed: 10613822]
5. Primo L, Ferrandi C, Roca C, et al. Identification of CD36 molecular features required for its in vitro angiostatic activity. Faseb J. 2005; 19:1713–1715. [PubMed: 16037098]
6. Abe T, Shimamura M, Jackman K, et al. Key role of CD36 in Toll-like receptor 2 signaling in cerebral ischemia. Stroke. 2010; 41:898–904. [PubMed: 20360550]
7. Stewart CR, Stuart LM, Wilkinson K, et al. CD36 ligands promote sterile inflammation through assembly of a Toll-like receptor 4 and 6 heterodimer. Nat Immunol. 2010; 11:155–161. [PubMed: 20037584]
8. Cho S, Park EM, Febbraio M, et al. The class B scavenger receptor CD36 mediates free radical production and tissue injury in cerebral ischemia. J Neurosci. 2005; 25:2504–2512. [PubMed: 15758158]
9. Park L, Wang G, Zhou P, et al. Scavenger receptor CD36 is essential for the cerebrovascular oxidative stress and neurovascular dysfunction induced by amyloid-beta. Proc Natl Acad Sci U S A. 2011; 108:5063–5068. [PubMed: 21383152]
10. Cho S, Szeto HH, Kim E, et al. A novel cell-permeable antioxidant peptide, SS31, attenuates ischemic brain injury by down-regulating CD36. J Biol Chem. 2007; 282:4634–4642. [PubMed: 17178711]
11. Zhao X, Sun G, Zhang J, et al. Hematoma resolution as a target for intracerebral hemorrhage treatment: role for peroxisome proliferator-activated receptor gamma in microglia/macrophages. Ann Neurol. 2007; 61:352–362. [PubMed: 17457822]
12. Zhao X, Grotta J, Gonzales N, Aronowski J. Hematoma resolution as a therapeutic target: the role of microglia/macrophages. Stroke. 2009; 40:S92–94. [PubMed: 19064796]
13. Mackay MT, Wiznitzer M, Benedict SL, et al. Arterial ischemic stroke risk factors: the International Pediatric Stroke Study. Ann Neurol. 2011; 69:130–140. [PubMed: 21280083]
14. Vexler ZS, Yenari MA. Does inflammation after stroke affect the developing brain differently than adult brain? Dev Neurosci. 2009; 31:378–393. [PubMed: 19672067]
15. Ikonomidou C, Bosch F, Miksa M, et al. Blockade of NMDA receptors and apoptotic neurodegeneration in the developing brain. Science. 1999; 283:70–74. [PubMed: 9872743]
16. Sheldon RA, Jiang X, Francisco C, et al. Manipulation of antioxidant pathways in neonatal murine brain. Pediatr Res. 2004; 56:656–662. [PubMed: 15295091]
17. Faustino J, Wang X, Jonhson C, et al. Microglial cells contribute to endogenous brain defenses after acute neonatal focal stroke. J Neurosci. 2011; 31:12992–13001. [PubMed: 21900578]
18. Han BH, Xu D, Choi J, et al. Selective, reversible caspase-3 inhibitor is neuroprotective and reveals distinct pathways of cell death following neonatal hypoxic- ischemic brain injury. J Biol Chem. 2002; 277:30128–30136. [PubMed: 12058036]
19. Manabat C, Han BH, Wendland M, et al. Reperfusion differentially induces caspase-3 activation in ischemic core and penumbra after stroke in immature brain. Stroke. 2003; 34:207–213. [PubMed: 12511776]
20. Stolzing A, Grune T. Neuronal apoptotic bodies: phagocytosis and degradation by primary microglial cells. Faseb J. 2004; 18:743–745. [PubMed: 14766802]
21. Lucas M, Stuart LM, Zhang A, et al. Requirements for apoptotic cell contact in regulation of macrophage responses. J Immunol. 2006; 177:4047–4054. [PubMed: 16951368]
22. Derugin N, Ferriero DM, Vexler ZS. Neonatal reversible focal cerebral ischemia: a new model. Neurosci Res. 1998; 32:349–353. [PubMed: 9950062]
23. Derugin N, Dingman A, Wendland M, et al. Magnetic Resonance Imaging as a Surrogate Measure for Histological Sub-Chronic Endpoint in a Neonatal Rat Stroke Model. Brain Res. 2005; 1066:49–56. [PubMed: 16336947]
24. Denker S, Ji S, Lee SY, et al. Macrophages are Comprised of Resident Brain Microglia not Infiltrating Peripheral Monocytes Acutely after Neonatal Stroke. J Neurochem. 2007; 100:893–904. [PubMed: 17212701]

25. Albert ML, Pearce SF, Francisco LM, et al. Immature dendritic cells phagocytose apoptotic cells via alphavbeta5 and CD36, and cross-present antigens to cytotoxic T lymphocytes. J Exp Med. 1998; 188:1359–1368. [PubMed: 9763615]
26. Lauber K, Bohn E, Krober SM, et al. Apoptotic cells induce migration of phagocytes via caspase-3-mediated release of a lipid attraction signal. Cell. 2003; 113:717–730. [PubMed: 12809603]
27. Moore KJ, El Khoury J, Medeiros LA, et al. A CD36-initiated signaling cascade mediates inflammatory effects of beta-amyloid. J Biol Chem. 2002; 277:47373–47379. [PubMed: 12239221]
28. Stuart LM, Bell SA, Stewart CR, et al. CD36 signals to the actin cytoskeleton and regulates microglial migration via a p130Cas complex. J Biol Chem. 2007; 282:27392–27401. [PubMed: 17623670]
29. Mallat M, Marin-Teva JL, Cheret C. Phagocytosis in the developing CNS: more than clearing the corpses. Curr Opin Neurobiol. 2005; 15:101–107. [PubMed: 15721751]
30. Hu BR, Liu CL, Ouyang Y, et al. Involvement of caspase-3 in cell death after hypoxia-ischemia declines during brain maturation. J Cereb Blood Flow Metab. 2000; 20:1294–1300. [PubMed: 10994850]
31. Ravichandran KS, Lorenz U. Engulfment of apoptotic cells: signals for a good meal. Nat Rev Immunol. 2007; 7:964–974. [PubMed: 18037898]
32. Helming L, Winter J, Gordon S. The scavenger receptor CD36 plays a role in cytokine-induced macrophage fusion. J Cell Sci. 2009; 122:453–459. [PubMed: 19155290]
33. Hoosdally SJ, Andress EJ, Wooding C, et al. The Human Scavenger Receptor CD36: glycosylation status and its role in trafficking and function. J Biol Chem. 2009; 284:16277–16288. [PubMed: 19369259]
34. Kim E, Tolhurst AT, Qin LY, et al. CD36/fatty acid translocase, an inflammatory mediator, is involved in hyperlipidemia-induced exacerbation in ischemic brain injury. J Neurosci. 2008; 28:4661–4670. [PubMed: 18448643]
35. Coraci IS, Husemann J, Berman JW, et al. CD36, a class B scavenger receptor, is expressed on microglia in Alzheimer's disease brains and can mediate production of reactive oxygen species in response to beta-amyloid fibrils. Am J Pathol. 2002; 160:101–112. [PubMed: 11786404]
36. Wilkinson B, Koenigsknecht-Talboo J, Grommes C, et al. Fibrillar beta-amyloid-stimulated intracellular signaling cascades require Vav for induction of respiratory burst and phagocytosis in monocytes and microglia. J Biol Chem. 2006; 281:20842–20850. [PubMed: 16728400]
37. Kunz A, Abe T, Hochrainer K, et al. Nuclear factor-kappaB activation and postischemic inflammation are suppressed in CD36-null mice after middle cerebral artery occlusion. J Neurosci. 2008; 28:1649–1658. [PubMed: 18272685]
38. Doverhag C, Keller M, Karlsson A, et al. Pharmacological and genetic inhibition of NADPH oxidase does not reduce brain damage in different models of perinatal brain injury in newborn mice. Neurobiol Dis. 2008; 31:133–144. [PubMed: 18571099]
39. Fullerton HJ, Ditelberg JS, Chen SF, et al. Copper/zinc superoxide dismutase transgenic brain accumulates hydrogen peroxide after perinatal hypoxia ischemia. Ann Neurol. 1998; 44:357–364. [PubMed: 9749602]
40. Bamberger ME, Harris ME, McDonald DR, et al. A cell surface receptor complex for fibrillar beta-amyloid mediates microglial activation. J Neurosci. 2003; 23:2665–2674. [PubMed: 12684452]
41. Resh MD. Myristylation and palmitylation of Src family members: the fats of the matter. Cell. 1994; 76:411–413. [PubMed: 8313462]
42. Sato I, Obata Y, Kasahara K, et al. Differential trafficking of Src, Lyn, Yes and Fyn is specified by the state of palmitoylation in the SH4 domain. J Cell Sci. 2009; 122:965–975. [PubMed: 19258394]
43. Luciano F, Ricci JE, Auberger P. Cleavage of Fyn and Lyn in their N-terminal unique regions during induction of apoptosis: a new mechanism for Src kinase regulation. Oncogene. 2001; 20:4935–4941. [PubMed: 11526478]

44. Thorne RF, Law EG, Elith CA, et al. The association between CD36 and Lyn protein tyrosine kinase is mediated by lipid. Biochem Biophys Res Commun. 2006; 351:51–56. [PubMed: 17052693]

45. Nijboer CH, Heijnen CJ, Groenendaal F, et al. Strong neuroprotection by inhibition of NF-kappaB after neonatal hypoxia-ischemia involves apoptotic mechanisms but is independent of cytokines. Stroke. 2008; 39:2129–2137. [PubMed: 18420952]

46. Nijboer CH, Heijnen CJ, Groenendaal F, et al. A dual role of the NF-kappaB pathway in neonatal hypoxic-ischemic brain damage. Stroke. 2008; 39:2578–2586. [PubMed: 18420947]

47. Fernandez Lopez D, Faustino J, Daneman R, et al. Blood-brain barrier permeability is increased after acute adult stroke but not neonatal stroke. J Neurosci. 2012 in press.

48. Ingley E. Src family kinases: regulation of their activities, levels and identification of new pathways. Biochim Biophys Acta. 2008; 1784:56–65. [PubMed: 17905674]

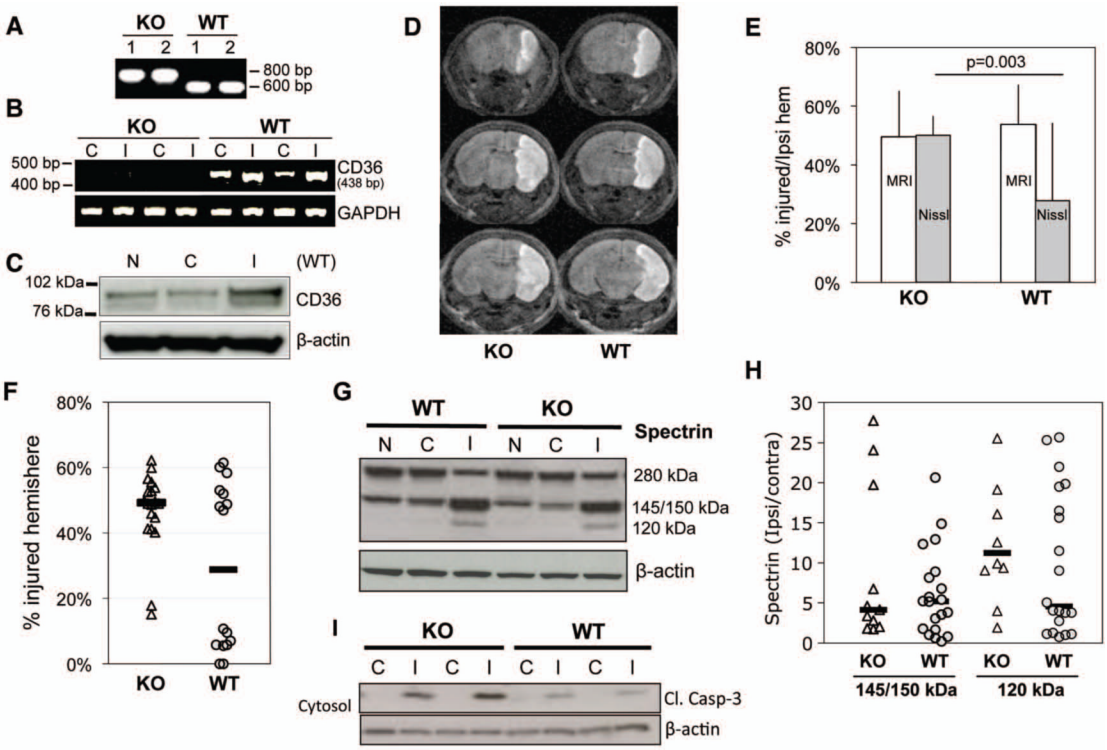

Figure 1. DWI lesions are similar in P9 WT and CD36ko mice during MCAO but injury is more severe in CD36ko than in WT mice 24 hours after reperfusion

A. Representative examples of genotyping of CD36ko and WT mice. A DNA band of 540bp represents WT allele and a DNA band of 780bp represents a KO allele. **B**. RT-PCR CD36 transcript is seen in WT but not in CD36ko mice. Note that CD36 transcription is increased in injured tissue of WT mice. **C**. Western blot analysis demonstrating that CD36 protein expression is increased in injured tissue. **D-F**. D. A representative example of DWI 2.5 hour after MCAO. E. Volume of DWI-identifiable injury during MCAO is similar in CD36ko and WT mice. At 24 hrs, infarct volume is significantly smaller in WT than in CD36ko mice. *p < 0.03 (n=10-11 per group). **F**. Infarct volume in individual mice subjected to 3 hours of MCAO. Shown are values for individual mice. Black bars – medians. **G-H**. Calpain- and caspase-3 mediated spectrin cleavage. G. Representative examples of Western blot analysis. 280kDa band – uncleaved spectin; 145/150kDa band – calpain-cleaved spectrin; 120kDa – caspase-3-cleaved spectrin. **H**. Data for individual mice. Black bars – medians. **I**. Protein expression of cl.casp-3 (17kDa fragment) in the cytosol. Shown are values for individual mice. Black bars – medians.

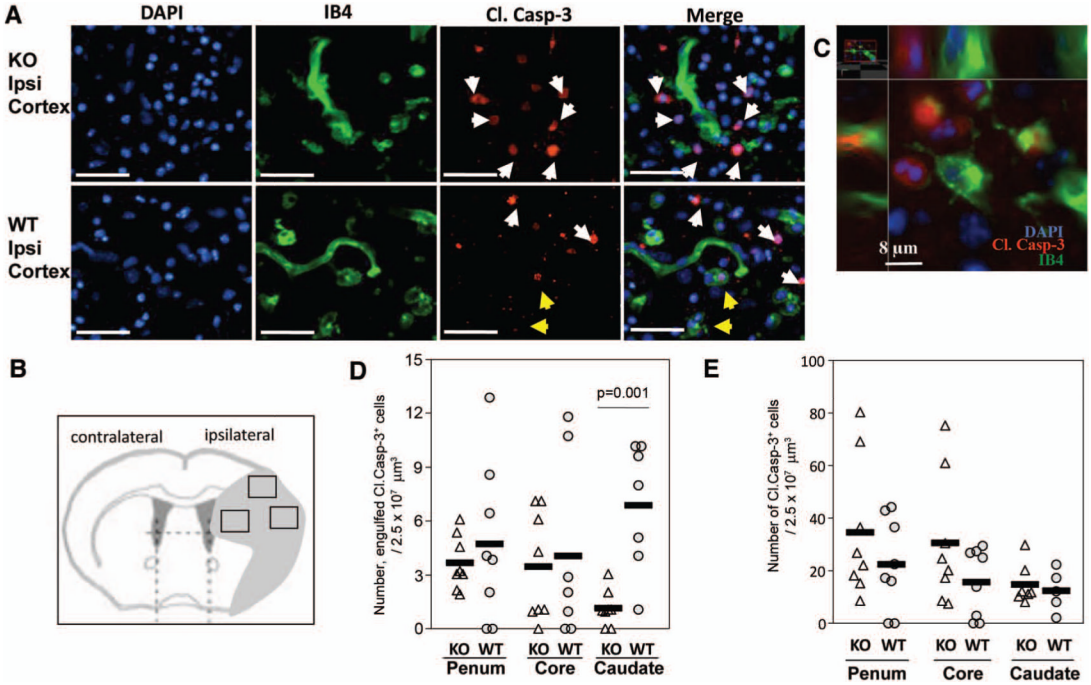

Figure 2. Phagocytosis of cells with Cl.casp-3 in the injured cortex is adversely affected by genetic deletion of CD36 at 24 hr of reperfusion

A. Representative images showing that cl.casp-3$^+$ (red) cells are seen in injured regions of both CD36ko and WT mice, a subpopulation of cl.casp-3$^+$ is engulfed in activated microglial cells of WT but not CD36ko mice. Some apoptotic cells are phagocytosed to microglia/macrophages. **B**. A diagram showing FOV for measurements. **C**. High magnification images of cells expressing cl.casp-3$^+$ distant from or engulfed by activated microglia. **D**. The number of cl.casp-3$^+$ engulfed by IB4$^+$ activated microglia in injured caudate is significantly higher in WT than in CD36ko mice. **E**. The number of cl.casp-3$^+$ cells. Shown are values for individual mice. Black bars – medians.

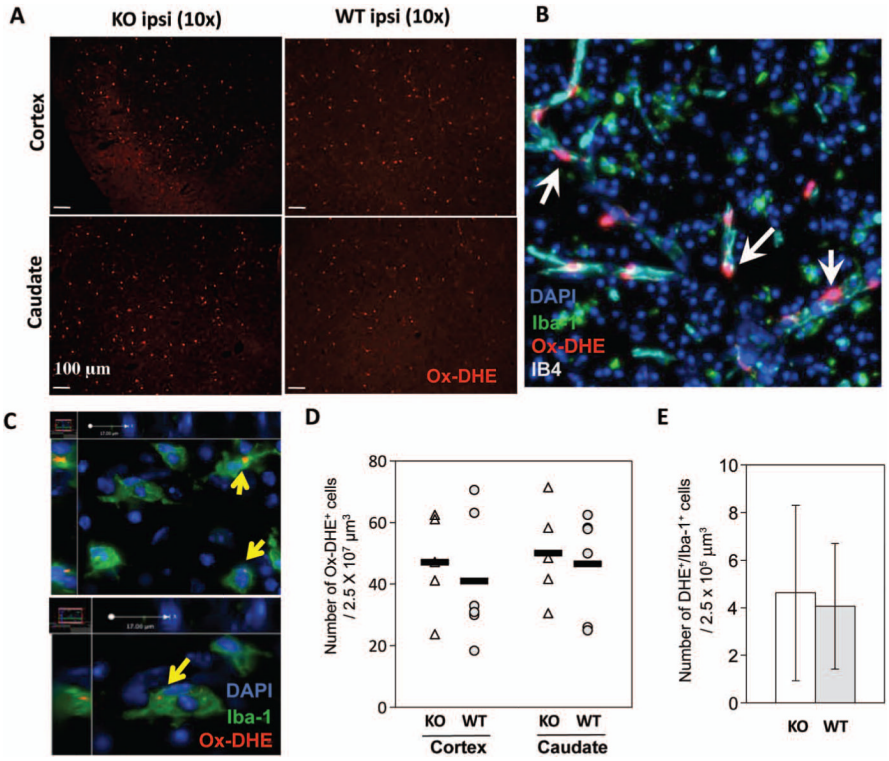

Figure 3. Superoxide accumulation is similar in P9 WT and CD36ko mice 24 hours after MCAO

A-C. Representative examples of low (A) and high (B) magnification images of Ox-DHE$^+$ cells in injured cortex and caudate of WT (n=6) and CD36ko pups (n=5). White arrows - Ox-DHE$^+$ cells associated with the vasculature; yellow arrows - dotted Ox-DHE$^+$ signal within activated microglia. **D-E**. D. The total number of Ox-DHE$^+$ cells. E. Ox-DHE$^+$ signal was observed only in a small fraction of Iba1$^+$microglia (WT, n=4, 14 FOV; KO n=4, measurements performed in 11 FOV).

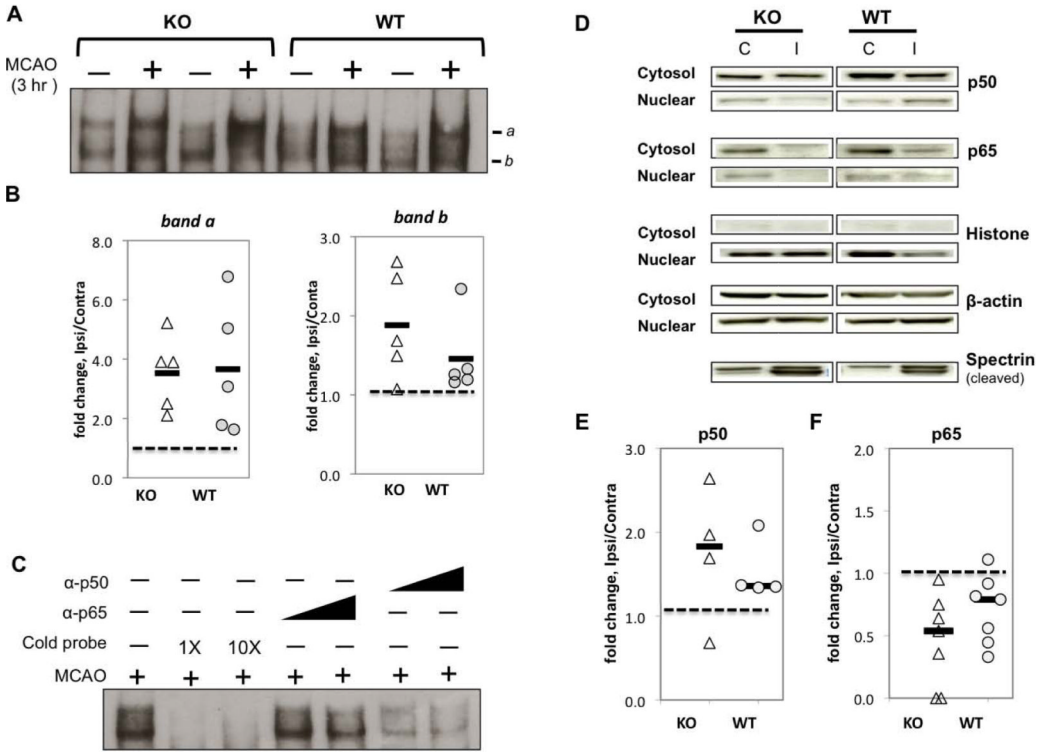

Figure 4. NF-κB activation is not suppressed in neonatal CD36ko mice 24 hours after MCAO

A. A representative example of NF-κB binding activity in contralateral and injured tissue (confirmed by spectin cleavage) in neonatal WT and CD36ko subjected to 3 hour MCAO. Shown are values for individual mice. Black bars – medians. **B**. Summarized data from panel A are presented as a ratio of injured/contralateral tissue. **C**. Competition assay (three lanes on the left): The disappearance of bands *a* and *b* in the presence of an unlabeled NFκB probe confirms the specificity. Supershift assay (four lanes on the right): A partial dose-dependent suppression of NFκB binding is seen in the presence of anti-p65 and anti-p50 antibodies. **D**. Western blot analysis of p65 and p50 in the cytosolic and nuclear fractions from injured regions (evident from cleaved spectrin). Purity of the cytosolic and nuclear fractions was confirmed by probing for histone H1. Dashed line demarcates expression in the contralateral hemisphere in the same rats. **E**. Quantification of p50 expression in the nucleus. **F**. Quantification of p65 expression in the nucleus.

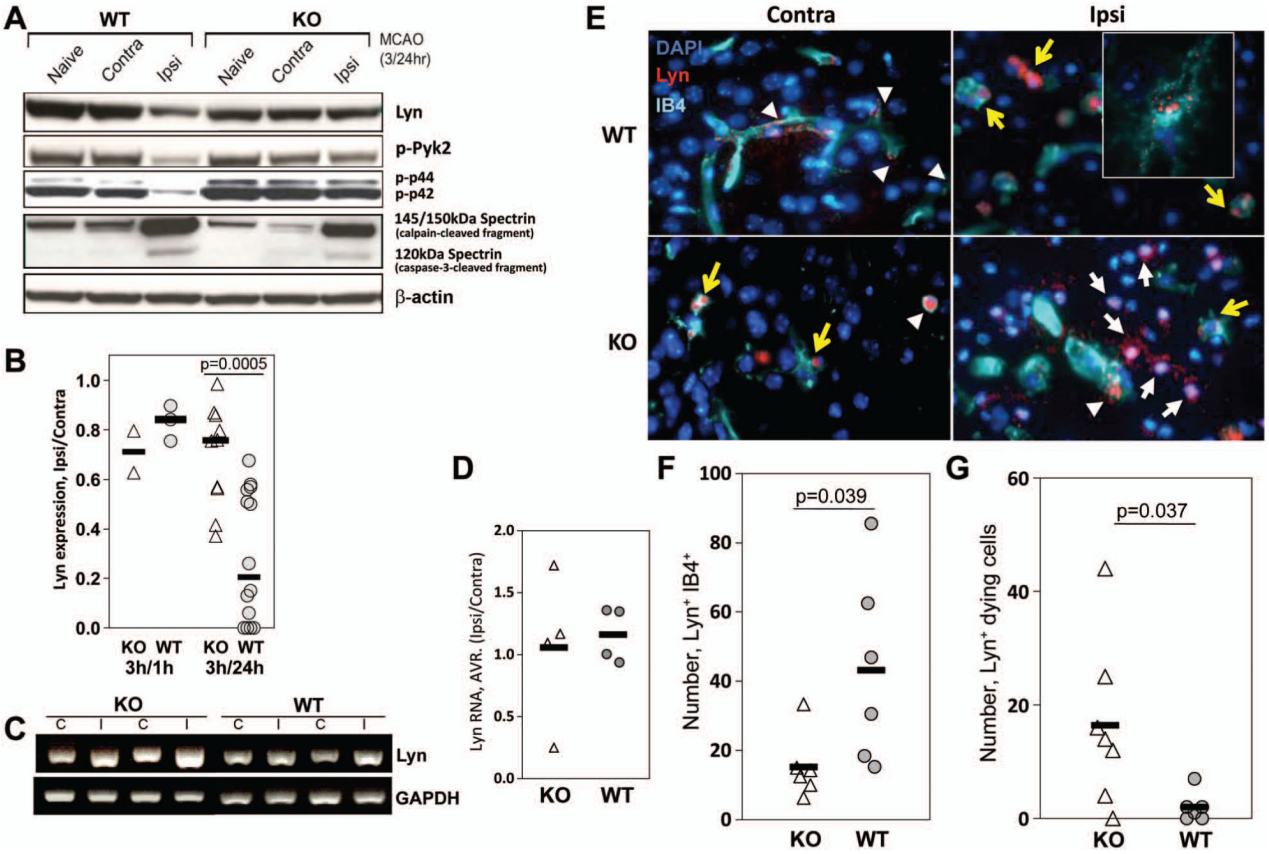

Figure 5. Genetic deletion of CD36 markedly alters both the expression and cell-type specific localization of Lyn in neonatal injured mice

A. A representative example of Western blot in whole cell lysate (WCL) at 24 hours following a 3 hour MCAO. **B**. Lyn expression in injured brain regions of individual rats (injury confirmed by spectin cleavage) is shown as a ratio of expression in ipsilateral/ contralateral tissue (Western blot analysis; WCL, data normalized to β-actin expression). Lyn expression was unchanged 1 hour after reperfusion (bars in the Left). Lyn expression was significantly reduced in injured regions of WT mice but was relatively preserved in CD36ko mice 24 hr after reperfusion (bars on the Right). **C-D**. Transcriptional levels of Lyn (C). Data quantification in C (D). **E**. Representative examples of Lyn immunoreactivity (red) in WT and CD36ko 24 hr after reperfusion. Lyn is localized in the vessels and microglia/macrophages ($IB4^+$) of contralateral hemisphere of WT (n=6) and KO (n=7) and is predominantly present in apoptotic cells ($DAPI^+$, blue) of ipsilateral hemisphere of KO not WT. **F-G**. Quantification of the number of $Lyn^+/IB4^+$ microglial cells (F) and Lyn^+ dying cells (G). n=6/group. F. Compared to WT, the number of $IB4^+$ cells that expressed Lyn (see Supplementary Methods for selection criteria) was significantly low in CD36ko than in WT. **G**. Lyn expression was rarely seen in cells with abnormally looking $DAPI^+$ nuclei in WT, but the number of such cells was significantly higher in CD36ko. Values are per 2.5×10^7 um^3 voxel.